Original Paper

Cellular Physiology and Biochemistry

Cell Physiol Biochem 2011;28:715-724

Accepted: September 19, 2011

CFTR and TMEM16A are Separate but Functionally Related Cl^- Channels

Jiraporn Ousingsawat#, Patthara Kongsuphol#, Rainer Schreiber and Karl Kunzelmann

Institut für Physiologie, Universität Regensburg, Regensburg, #JO and PK share first authorship

Key Words

Ca^{2+} activated Cl^- currents • CaCC • TMEM16A • CFTR • Cystic fibrosis • CF

Abstract

Previous reports point out to a functional relationship of the cystic fibrosis transmembrane conductance regulator (CFTR) and Ca^{2+} activated Cl^- channels (CaCC). Recent findings showing that TMEM16A forms the essential part of CaCC, prompted us to examine whether CFTR controls TMEM16A. Inhibition of endogenous CaCC by activation of endogenous CFTR was found in 16HBE human airway epithelial cells, which also express TMEM16A. In contrast, CFBE airway epithelial cells lack of CFTR expression, but express TMEM16A along with other TMEM16-proteins. These cells produce CaCC that is inhibited by overexpression and activation of CFTR. In HEK293 cells coexpressing TMEM16A and CFTR, whole cell currents activated by IMBX and forskolin were significantly reduced when compared with cells expressing CFTR only, while the halide permeability sequence of CFTR was not changed. Expression of TMEM16A, but not of TMEM16F, H or J, produced robust CaCC, which that were inhibited by CaCCinh-A01 and niflumic acid, but not by CFTRinh-172. TMEM16A-currents were attenuated by additional expression of CFTR, and were completely abrogated when additionally expressed CFTR was activated by IBMX and forskolin. On the other hand, CFTR-currents were attenuated by additional expression of TMEM16A. CFTR and TMEM16A were both membrane localized and could be coimmuno-precipitated. Intracellular Ca^{2+} signals elicited by receptor-stimulation was not changed during activation of CFTR, while ionophore-induced rise in $[Ca^{2+}]_i$ was attenuated after stimulation of CFTR. The data indicate that both CFTR and TMEM16 proteins are separate molecular entities that show functional and molecular interaction.

Copyright © 2011 S. Karger AG, Basel

Introduction

The cystic fibrosis transmembrane conductance regulator (CFTR) is regarded as a cAMP/PKA/ATP-regulated Cl^- channel that also controls the function of other membrane proteins [1]. Apart from the well examined effects of CFTR on epithelial Na^+ conductance, it has also been reported earlier that CFTR inhibits

KARGER

Fax +41 61 306 12 34
E-Mail karger@karger.ch
www.karger.com

© 2011 S. Karger AG, Basel
1015-8987/11/0284-0715$38.00/0

Accessible online at:
www.karger.com/cpb

Karl Kunzelmann
Institut für Physiologie, Universität Regensburg
Universitätsstraße 31, 93053 Regensburg (Germany)
Tel. +49 (0)941 943 4302, Fax +49 (0)941 943 4315
E-Mail karl.kunzelmann@vkl.uni-regensburg.de

endogenous Ca^{2+} activated Cl^- currents (CaCC) in *Xenopus* oocytes, bovine pulmonary artery endothelium and isolated parotid acinar cells, by an yet unknown mechanism [2-5]. Moreover, also volume-regulated anion channels were inhibited by expression of CFTR [6]. Additional studies demonstrated that upregulation or downregulation of CFTR resulted in a parallel up- and downregulation of cAMP-, Ca^{2+}-, and volume regulated Cl^- conductance [7]. Although these data suggested a functional and even molecular relationship of different anion conductances, they are regarded as separate molecular entities [8].

Another line of evidence, indicating the relationship of CFTR and CaCC, came from the observation that CaCC is augmented in airways of patients suffering from cystic fibrosis. Thus purinergic peak secretory response was enhanced in cultured CF airway epithelial cells as well as freshly excised nasal tissues from CF patients [9, 10]. Also in nasal epithelial of CF mice, enhanced Ca^{2+} dependent Cl^- secretion was detected [11]. It was concluded that expression levels for alternative Ca^{2+} dependent Cl^- channels are an important determinant of the severity of CF [12]. Also in the intestinal epithelium of CFTR-deficient mice that were generated by backcrossing and intercrossing of progenies with different inbred strains, prolonged survival was observed that was paralleled by up-regulation of CaCC [13].

In the previous search for modifiers of disease severity of cystic fibrosis, the CLCA gene locus was identified as a modulator of the gastrointestinal basic defect in CF [14]. Although the role of CLCA for Ca^{2+} dependent Cl^- conductance remains illusive, its role during inflammatory airway disease is clearly emerging [15, 16]. However, CLCA proteins are probably not independent CaCCs, but may contribute to the activity of the actual membrane localized CaCC. Notably, hClCa1 has been shown to elevate the single channel conductance of endogenous Ca^{2+} dependent Cl^- channels by lowering the energy barriers for ion translocation through the pore [17].

Recently TMEM16A has been identified as CaCC by three independent groups [18-20]. TMEM16A knockout animals have severe transport defects in various epithelial tissues, including the airways [21, 22]. Since Ca^{2+}-dependent Cl^- channels, or at least a major component of it, have now been identified, we examined the functional relationship between TMEM16A and CFTR and aimed to identify the mechanism by which CFTR may affect TMEM16A. Our experiments suggest that CFTR controls Ca^{2+} dependent Cl^- secretion by inhibiting TMEM16A.

Materials and Methods

Cell culture, RT-PCR

CFBE41o-, 16HBE, and CFBE41o- cells stably expressing wild-type CFTR [23] were generous gifts from Dr. D. Gruenert (Univ. California San Francisco, USA) and Dr. J.P. Clancy (Univ. of Alabama at Birmingham, USA) and were grown in Minimum Essential Medium supplemented with 2 mM glutamine. Human embryonic kidney (HEK293) cells were grown in Dulbecco's modified Eagle's medium. All media were supplemented 10% fetal calf serum. Cells were incubated in 5% CO_2 at 37°C. Expression of mRNAs encoding all 10 human TMEM16 proteins was examined in CFBE41o- cells by standard RT-PCR using primers as described in [24].

cDNAs, siRNA, real time RT-PCR and transfection

cDNA for human TMEM16A, F, and J were amplified from total RNA of 16HBE and CFBE cells by RT-PCR, as recently described [25]. In brief: Real-time PCR was performed in a Light Cycler (Roche), using the Quanti Tect SYBR Green PCR Kit (Qiagen, Hilden, Germany). Each reaction contained 2 µl Master Mix (including *Taq* polymerase, DNTPs, SYBR green buffer), 1 pM of each primer sense and anti-sense, 2.5 mM $MgCl_2$, and 2 µl cDNA. After activation of the Taq polymerase for 10 min at 94° cDNA was amplified by 15 s at 94°C, 10 s at 55°C, and 20 s at 72°C, for 50 cycles. The amplification was followed by a melting curve analysis to control of the PCR products. The primer sequences were: hTMEM16A: (NM_018043.4): 5'-CCT CAC GGG CTT TGA AGA G-3', 5'-CTC CAA GAC TCT GGC TTC GT-3'; hTMEM16F: (NM_001025356.1): 5'-AGG AAT GTT TTG CTA CAA ATG GA-3', 5'-GTC CAA GGT TTT CCA ACA CG-3'; hTMEM16H: NM_020959.1): 5'-GGA GGA CCA GCC AAT CAT C-3', 5'-TGC TCG TGG ACA GGG AAC-3'; hTMEM16J (NM_001012302.2): 5'-CAA ACC CCA GCT GGA ACT C-3', 5'-GGA TCC GGA GGC TCT CTT-3'. Analysis of the data was performed using Light Cycler software 3.5.3. Standard curves for TMEMs mRNA and β-actin mRNA were produced by using cDNA of transfected HEK cells at different dilutions. The ratio of the amount of TMEM to β-actin mRNA was calculated for each sample and analysis was performed in triplicates. TMEM16A-K610A was produced by PCR-based site-directed mutagenesis. Human TMEM16H was purchased from imaGenes (Clone:IMAGp998FF0411661Q, Berlin, Germany). The cDNAs were subcloned into pcDNA3.1 V5-His (Invitrogen, Karlsruhe, Germany). For immunocytochemistry and co-immunoprecipitation, TMEM16A was tagged with EGFP. Wild-type CFTR was tagged with FLAG as described earlier [26], and was introduced into pmCherry-C2 vector. Expression of TMEM16A, TMEM16F, TMEM16H, and TMEM16J were suppressed by two to three independent sets of siRNA. Duplexes of 25 nucleotides of siRNA were designed (5' target regions) and synthesized by Invitrogen and Santa Cruz. Plasmids or siRNA were transfected into CFBE cells stably expressing wtCFTR, or HEK293 cells (transient expression), using standard methods (Lipofectamine, Invitrogen), and cells were examined 48 or 72 h after transfection. The siRNA sequence were: 16A: 5´-AAG UUA GUG AGG UAG GCU GGG AAC C-3'; 16F: 5´-AUC ACA UGC CAA UAG UAG AUG UUG U-3'; 16H:

5´-GCU UCU CCU GCG AGG AGG ACU UUA U-3'; 16J: sc-96721(Santa Cruz Biotechnology).

Patch Clamping

Cells grown on cover slips were mounted in a perfused bath on the stage of an inverted microscope (IM35, Zeiss) and kept at 37°C The bath was perfused continuously with Ringer solution (mM: NaCl 145, KH_2PO_4 0.4, K_2HPO_4 1.6, d-glucose 6, $MgCl_2$ 1, Ca-gluconate 1.3, pH 7.4) at about 10 ml/min. NaCl was replaced by NaBr, NaI or NaSCN. Patch-clamp experiments were performed in the fast whole-cell configuration. Patch pipettes had an input resistance of 4-6 MΩ, when filled with an intracellular like solution containing (mM) KCl 30, K-gluconate 95, NaH_2PO_4 1.2, Na_2HPO_4 4.8, EGTA 1, Ca-gluconate 0.758, $MgCl_2$ 1.034, D-glucose 5, ATP 3. pH was 7.2, the Ca^{2+} activity was 0.1 µM. The access conductance was measured continuously and was 90-140 nS (EPC 9 amplifier, List Medical Electronics, Darmstadt, Germany). In regular intervals, membrane voltages (V_c) were clamped in steps of 10 mV from -100 to +100 mV and the membrane conductance G_m was calculated from the measured current (I) and V_c values according to Ohm's law.

Immunohistochemistry

GFP tagged TMEM16A and CFTR-Cherry coexpressing HEK293 cells were grown on glass cover slips. Nuclei were stained with Hoe33342 (0.1 µg/ml Ringer, Aplichem, Darmstadt, Germany) and examined as life images with an ApoTome Axiovert 200M fluorescence microscope (Zeiss, Göttingen, Germany). His-tagged TMEM16J and CFTR-Cherry transfected HEK293 cells were grown on glass cover slips and fixed for 10 min with 4% (w/v) paraformaldehyde at room temperature. Cells were permeabilized and blocked with 2% (w/v PBS) BSA and 0.04% (v/v PBS) Triton X-100 and incubated for 1 h with primary antibody mouse anti His tag (1:500, Qiagen, Hilden, Germany) at 37°C. Binding of the primary antibody was visualized by incubation with a secondary donkey anti-mouse antibodies conjugated with AlexaFluor®488 (1:1.000, Molecular Probes, Invitrogen). Nuclei were stained with Hoe33342 (0.1 µg/ml PBS, Aplichem, Darmstadt, Germany). Cells were mounted on glass slides with fluorescent mounting medium (DAKO Cytomation, Hamburg, Germany) and examined with an ApoTome Axiovert 200M fluorescence microscope (Zeiss, Göttingen, Germany). As a measure of co-localization between the signals in the red and green channels of confocal images, we calculated the Spearman's rank correlation coefficient using ImageJ PlugIn PSC-colocalization after background subtraction

Immunoprecipitation and Western blotting

Protein was isolated from CFBE or transfected HEK293 cells in lysis buffer containing 10mM HEPES, 2mM EDTA, 1% TritonX-100, 1% proteinase inhibitor cocktail and 5U/ml Benzonase. Prior to the addition of mouse monoclonal CFTR antibody (no. 570; CF Foundation Therapeutics) or GFP-antibody (SIGMA, Taufkirchen, Germany), protein lysates were precleared with protein G agarose beads (Pierce, Rockford, USA). Incubation of the precleared protein lysates with antibodies was performed overnight at 4°C, and the protein-antibody complex was immobilized with the addition of 20 µl of 50% slurry of protein G agarose beads for 2.5 h at 4°C. The beads were washed five times in wash buffer, and after the last washing step, beads were mixed in 2x Laemmli sample buffer for Western blot analysis. For Western blot analysis, the 10% SDS polyacrylamide gel was transferred to a polyvinylidene difluoride membrane (GE Healthcare EuropeGmbH, Munich, Germany) using wet transfer (BioRad, Munich, Germany). Membranes were incubated with anti-GFP rabbit antibodies (1:1,000, Molecular probe, Invitrogen) overnight at 4°C. Proteins were visualized using an anti-rabbit horseradish peroxidase (HRP)-conjugated antibody (1:10,000, Acaris) and blots were visualized using chemiliminescences (Pierce).

Measurement of the intracellular Ca^{2+} concentration

Transfected HEK293 cells were loaded with 5 µM Fura2-AM in Ringer solution at 37°C for 2 h. Fluorescence was detected at 37°C, using an inverted microscope IMT-2 (Olympus, Nürnberg, Germany) and a high speed polychromator system (VisiChrome, Puchheim, Germany). FFP-18 was excited at 340/380 nm, and emission was recorded between 470 and 550 nm using a CCD camera (CoolSnap HQ, Visitron). The results were obtained at 340/380 nm fluorescence ratio (after background subtraction).

Materials and statistical analysis

All compounds used were of high grade of purity and were from Sigma (Taufkirchen, Germany) or Merck (Darmstadt, Germany). The siRNAs were from Invitrogen and Santa Cruz Biotechnology, respectively). All cell culture reagents were from Invitrogen. Student's t-test (for paired or unpaired samples as appropriate), and analysis of variance (ANOVA) was used for statistical analysis. P values <0.05 were accepted as significant.

Results

CFTR inhibits TMEM16A/CaCC in human airways

Airway epithelial cell lines such as 16HBE14o- [27] and CFBE41o- [28] express endogenous CaCC. Similar to earlier experiments in *Xenopus* oocytes and mammalian cells [2-4], we found inhibition of CaCC after stimulation of CFTR in 16HBE14o- cells, which express both proteins endogenously [27, 29] (Fig. 1). To analyze the correlation between CaCC and CFTR in more detail, we examined expression of TMEM16-mRNA in CFBE/CFTR airway epithelial cells, which stably express CFTR as well as TMEM16A, F, H and J (Fig. 2A). In fact, a small but significant CaCC could be activated by purinergic stimulation with extracellular ATP (100 µM) (Fig. 2B). CFBE (parental) cells do not express wtCFTR and therefore do not generate Cl^- currents when stimulated with IBMX and forskolin (I/F) (Fig. 2B-D). In contrast, stably CFTR-transfected CFBE cells [23] demonstrate

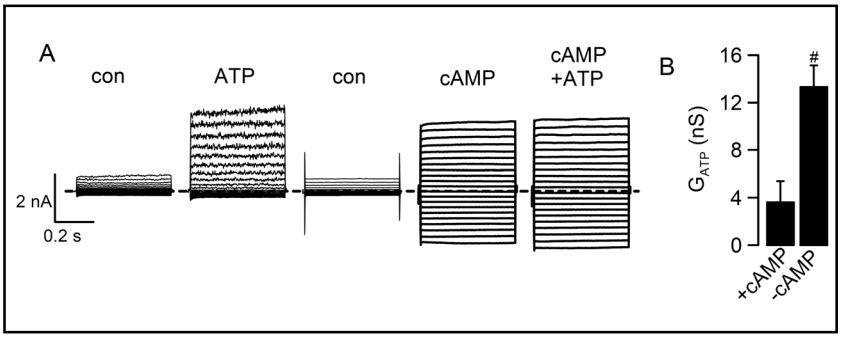

Fig. 1. Inhibition of endogenous CaCC by CFTR in 16HBE airway epithelial cells. A) Whole cell currents measured in human bronchial epithelial cells (16HBE14o-). ATP (100 μM) did not activate CaCC after stimulation of CFTR with IBMX (100 μM) and forskolin (2 μM). B) Summary of the ATP-induced whole cell conductances before and after stimulation of CFTR. Mean ± SEM, (n) = number of cells measured. #indicates significant difference compared to the presence of cAMP (unpaired t-test).

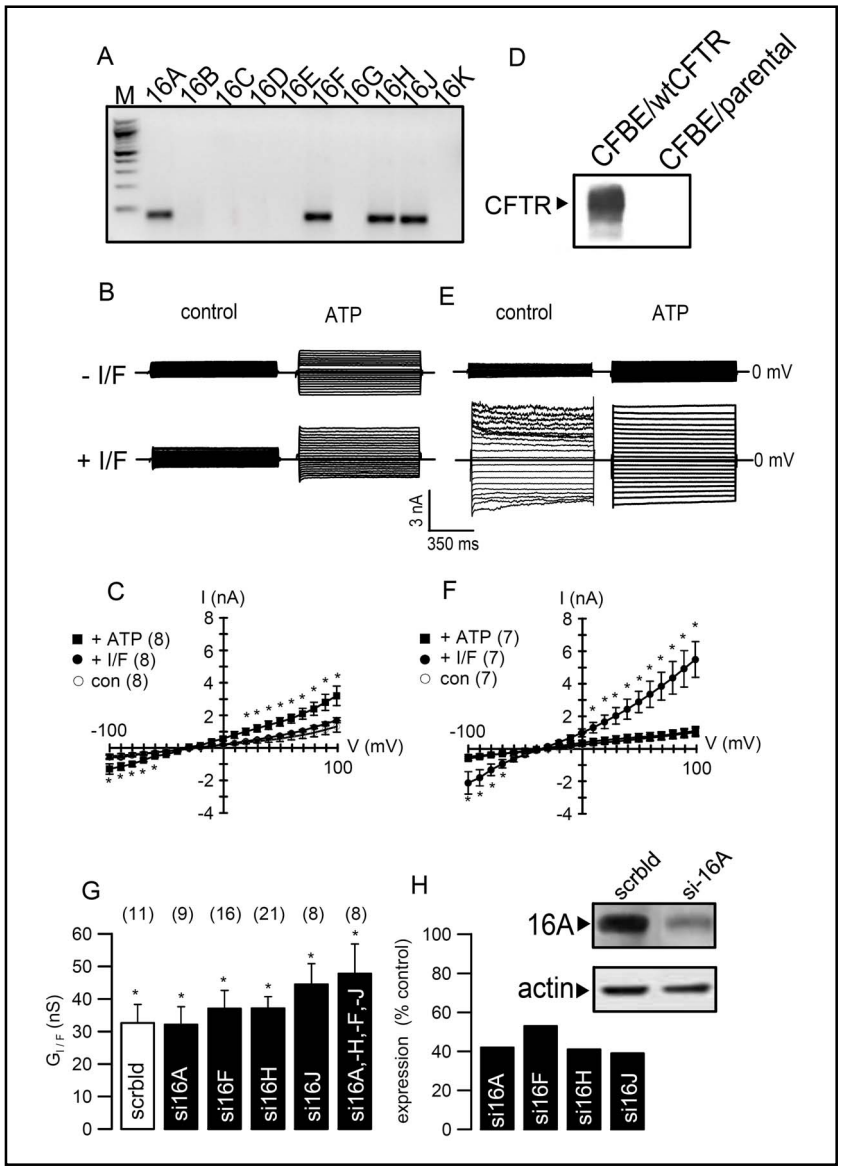

Fig. 2. Overexpression of CFTR inhibits endogenous CaCC in CFBE airway epithelial cells. A) RT-PCR analysis of 10 TMEM16-proteins endogenously expressed in CFBE41o- cells. B) Whole cell currents in CFBE parental cells in the absence or presence of ATP and I/F. C) Current voltage relationship obtained in CFBE41o- cells, and effects of ATP and I/F. D) Western blot of CFTR in CFBE parental cells and CFBE cells stably overexpressing CFTR. E) Whole cell currents in CFBE/CFTR cells in the absence or presence of ATP and I/F. F) Current voltage relationship obtained in CFBE cells, and effects of ATP and I/F. G) Whole cell conductances activated in CFBE/CFTR cells after incubation with different siRNAs (knockdown of TMEM16A, F, H, J) and scrambled RNA. H) Expression levels of mRNA for 4 different TMEM16 channels after siRNA treatment relative to cells treated with scrambled RNA, as detected by quantitative real time PCR. For TMEM16A, knockdown could also be demonstrated by Western blotting (insert). Mean ± SEM, (n) = number of cells measured. *significant current-activation by I/F (paired t-test).

I/F-activated whole cell currents, but lack of CaCC (Fig. 2D-F). Thus expression of CFTR appears to inhibit TMEM16A, although expression of TMEM16-proteins was not changed (data not shown). We also found that siRNA-suppression of TMEM16A reduced ATP-activated whole cell currents from 28±3.8 to 5.3±1.1 nS (n = 5), indicating that TMEM16A is essential for CaCC in human airway epithelial cells. Conversely, siRNA knockdown of TMEM16-proteins in CFBE/CFTR cells by two independent siRNAs did not change CFTR conductance (Fig. 2G,H) or its halide permeability (data not shown). Due to limited access to TMEM16-antibodies,

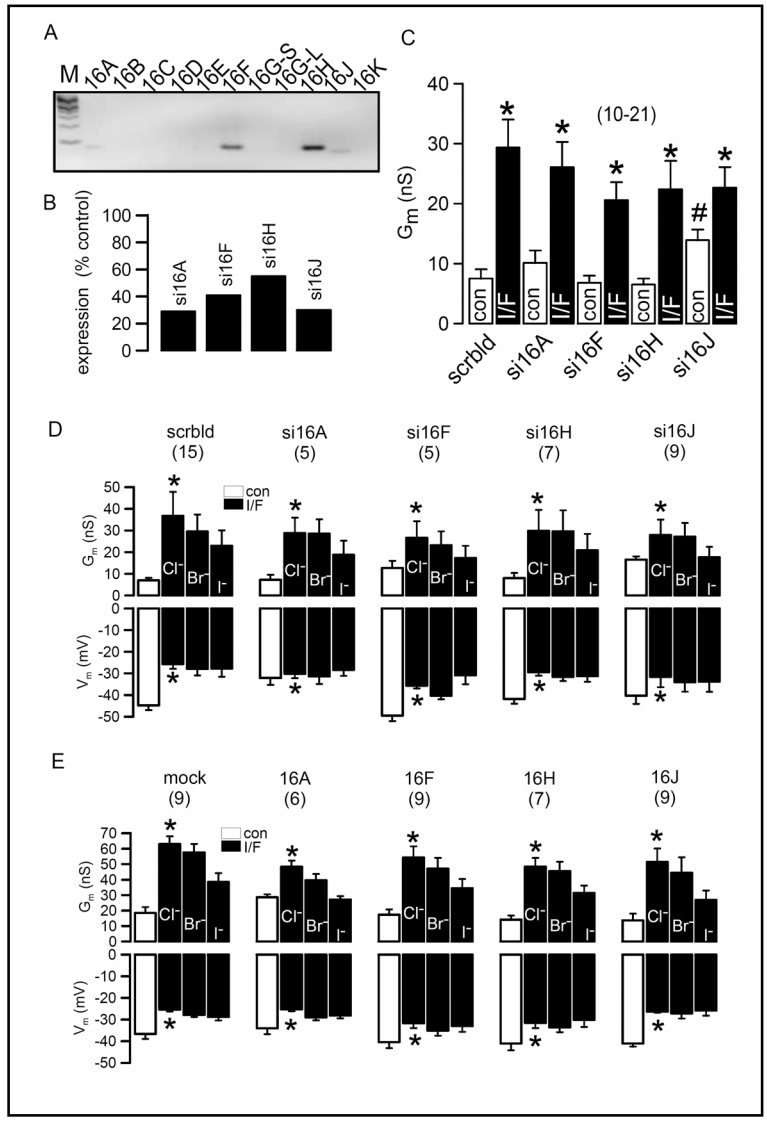

Fig. 3. CFTR-currents are largely independent of TMEM16-proteins: A) RT-PCR analysis of TMEM16-proteins expressed endogenously in HEK293 cells. B) Expression levels of mRNA for 4 different TMEM16 isoforms after siRNA treatment, relative to cells treated with scrambled RNA, as detected by quantitative real time PCR. C) Summary of the I/F induced changes in whole cell Cl^- conductance in HEK293 cells transiently expressing CFTR and treated with siRNA for TMEM16A, F, H, J and scrambled RNA. D) Summary of the whole cell conductances and membrane voltages measured in HEK293 cells transiently expressing CFTR and treated with siRNA for TMEM16A, F, H, J and scrambled RNA, in the presence of the extracellular halides Cl^-, Br^-, or I^-. E) Summary of the whole cell conductances and membrane voltages measured in HEK293 cells transiently coexpressing CFTR and TMEM16A, F, H, J, or empty plasmid (mock), in the presence of the extracellular halides Cl^-, Br^-, or I^-. Mean ± SEM, (n) = number of cells measured. *significant difference compared to absence of I/F (paired t-test). #significant difference compared to scrambled (unpaired t-test).

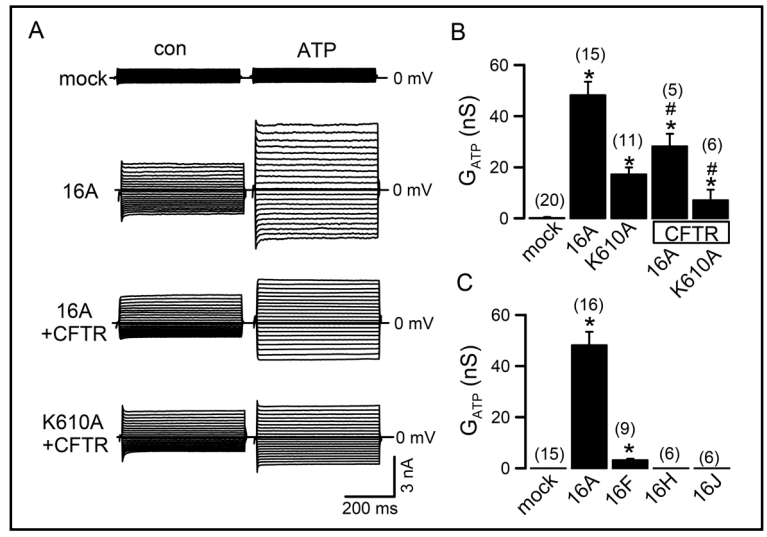

Fig. 4. Expression of CFTR inhibits TMEM16A-currents in HEK293 cells. A) Original recordings of whole cell currents and effect of ATP in HEK293 cells, transiently coexpressing CFTR and TMEM16A, TMEM16A-K610A, or empty plasmid. B) Summary of ATP-activated whole cell conductances in cells transiently expressing TMEM16A, TMEM16A-K610A, or coexpressing CFTR and TMEM16A or TMEM16A-K610A. Coexpression of CFTR inhibits TMEM16A. C) Summary of the ATP activated whole cell conductances in HEK293 cells overexpressing empty plasmid (mock), TMEM16A, F, H, J. Mean ± SEM, (n) = number of cells measured. *significant difference compared to mock (paired t-test).

we could verify knockdown by Western blotting only for TMEM16A (Fig. 2H - insert). Therefore knockdown was mainly demonstrated by quantitative real time RT-PCR (Fig. 2H). Taken together, our results show that i) TMEM16A forms CaCC in human airway epithelial cells, and ii) is inhibited CFTR.

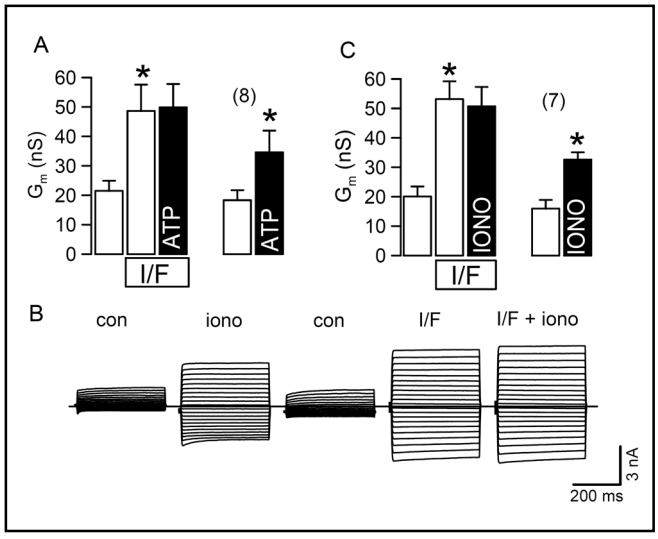

Fig. 5. Activation of CFTR inhibits TMEM16A-currents in HEK293 cells. A) Summary of whole cell conductances in cells transiently coexpressing CFTR and TMEM16A. Effects of stimulation with ATP after pre-activation of CFTR by I/F, or in the absence of I/F. No ATP-activated TMEM16A-currents were observed after stimulation of CFTR. B) Activation of whole cell currents by ionomycin (iono, 1 μM) in the absence or presence of pre-activation of CFTR by I/F. C) Summary of whole cell conductances in cells transiently coexpressing CFTR and TMEM16A. Effects of stimulation with ionomycin in the presence or absence of pre-activation of CFTR by I/F. No ionomycin-activated TMEM16A-currents were observed after stimulation of CFTR. Mean ± SEM, (n) = number of cells measured. *significant difference compared to control (paired t-test).

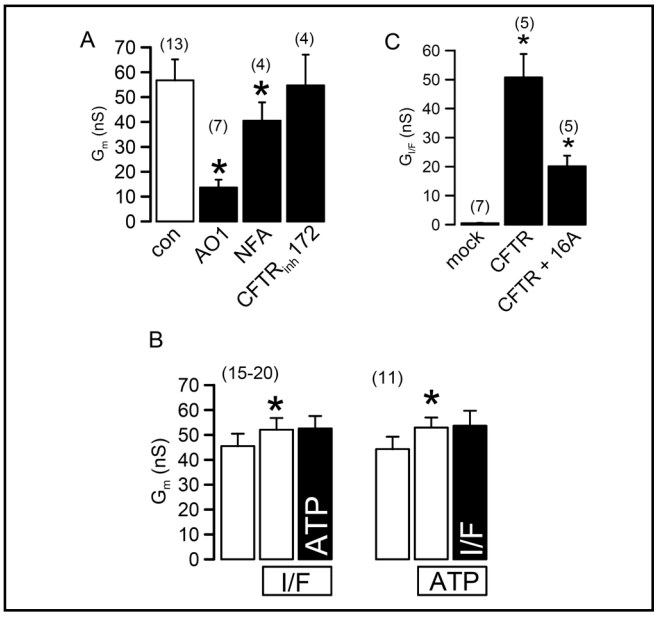

Fig. 6. Expression of TMEM16A inhibits CFTR in HEK293 cells. A) Summary of whole cell conductances in cells transiently coexpressing CFTR and TMEM16A, which demonstrate a large baseline conductance. The baseline conductance was inhibited by AO1 (20 μM), niflumic acid (10 μM) but not by $CFTR_{inh}172$ (5 μM). B) Summary of whole cell conductances in cells transiently coexpressing CFTR and TMEM16A, demonstrating a large baseline conductance. Effects of stimulation with I/F, ATP, or co-stimulation by I/F and ATP. C) I/F activated G indicates attenuation by coexpression of TMEM16A. Mean ± SEM, (n) = number of cells measured. *indicates significant difference compared to control (paired t-test).

CFTR-currents are largely independent of TMEM16-proteins

Additional experiments were performed in HEK293 cells transiently overexpressing wtCFTR. HEK293 cells express TMEM16F,H,J, and traces of TMEM16A and thus show very little CaCC [24] (Fig. 3A). Using two independent siRNAs, we knocked down expression of TMEM16-proteins individually (Fig. 3B), and measured CFTR whole cell conductances after stimulation with IBMX and forskolin. For TMEM16A, successful knockdown was verified by Western blotting. Because antibodies were not available for other TMEM16 proteins, knockdown was also demonstrated by real time RT-PCR [24] (Fig. 3B). siRNA did not affect CFTR-conductances except of siRNA for TMEM16J, which significantly increased the baseline conductance in HEK293 cells, and inhibited the IBMX/forskolin activated fraction, a result that is currently unexplained (Fig. 3C). However, the halide permeability sequence of I/F-activated CFTR currents remained essentially unchanged by siRNA-knockdown of the TMEM16 isoforms (Fig. 3D). Moreover, activation of CFTR and the halide-permeability sequence of CFTR-currents were not affected by coexpression of TMEM16-proteins together with CFTR. These results suggest that CFTR-currents are largely independent of TMEM16-proteins (Fig. 3E).

CFTR inhibits TMEM16A-currents in HEK293 cells

We examined TMEM16A-currents activated by the purinergic agonist ATP (100 μM) in HEK293 cells. While CaCC is negligible in control cells (mock), it's clearly detectable in cells expressing TMEM16A, or the pore mutant TMEM16A-K610A (Fig. 4A,B) [24]. Currents produced by TMEM16A and TMEM16A-K610A were attenuated in cells coexpressing CFTR (Fig. 4B). Notably only TMEM16A produced large Cl^- currents, while TMEM16F currents were very small. Overexpression of TMEM16H or TMEM16J did not produce any

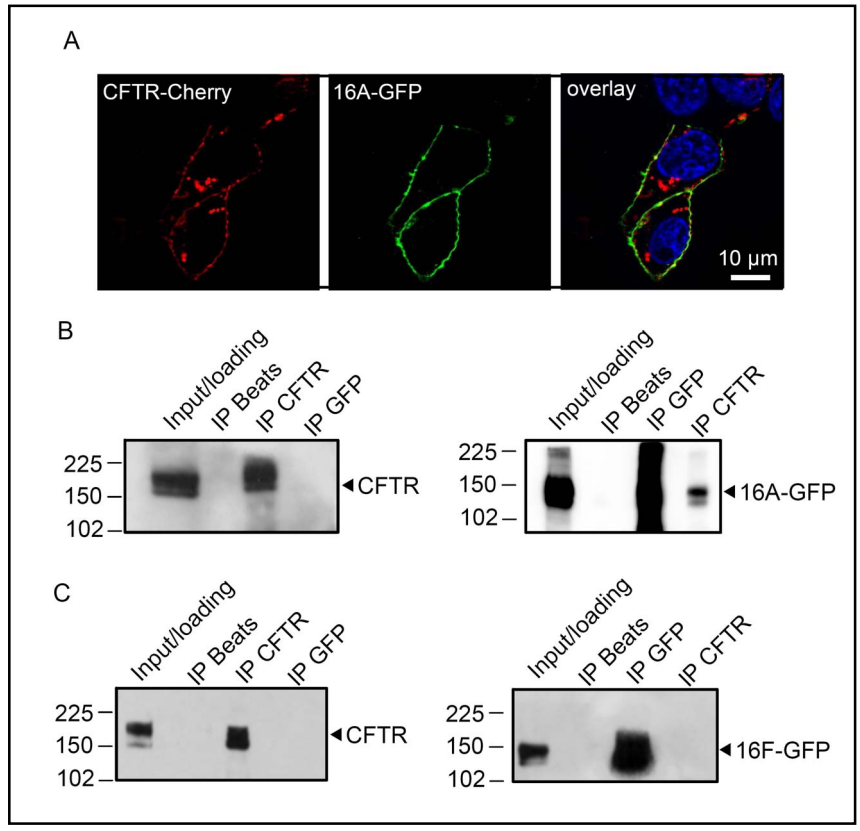

Fig. 7. Membrane localized CFTR and TMEM16A may physically interact: A) Immunocytochemistry (life imaging) of CFTR-Cherry (red; Cherry) and GFP tagged TMEM16A (GFP, green) when transiently overexpressed in HEK293 cells. Both CFTR and TMEM16A are clearly membrane localized. B) Coimmunoprecipitation of CFTR and TMEM16A-GFP. TMEM16A-GFP was detected using a GFP-antibody (input). Immunoprecipitation of beats only (no conjugated antibody) served as a control. TMEM16A-GFP was coimmunoprecipitated after pull-down of CFTR using CFTR-AB 596 (right panel), while CFTR was not coimmunoprecipitated with TMEM16A-GFP (left panel). C) Coimmunoprecipitation of CFTR and TMEM16F-GFP expressed in HEK293 cells. TMEM16F-GFP was not coimmunoprecipitated after pull-down of CFTR (right panel), while CFTR was not coimmunoprecipitated with TMEM16F-GFP (left panel). Input represents the loading control, i.e. amount of protein used for immunoprecipitation.

measureable currents, similar to an earlier study with FRT cells [25] (Fig. 4C). Moreover, after activation of CFTR, TMEM16A currents were completely inhibited (Fig. 5A).

Because receptor mediated Ca^{2+} signaling and activation of TMEM16A might be compromised during stimulation and activation of CFTR, we also examined whether receptor-independent activation of TMEM16A, by increase of Ca^{2+} through the Ca^{2+} ionophore ionomycin, was also affected by CFTR (Fig. 5B,C). In fact TMEM16A could no longer be activated by ionomycin after activation of CFTR. Notably, activation of whole cell Cl^- conductance by ATP (29.2±3.1, +I/F vs. 28.8±2.2, -I/F; n = 8) nS; or ionomycin (25.3±2.6, +I/F vs. 26.1±2.6, -I/F; n = 7) nS; were independent of I/F in cells expressing TMEM16A only. Interestingly, cells overexpressing TMEM16A show a higher baseline conductance that was inhibited by 20 µM of the CaCC inhibitor AO1 [30] or niflumic acid (NFA; 10 µm), but not by $CFTR_{inh}172$, indicating partially active TMEM16A even at baseline $[Ca^{2+}]_i$ levels (Fig. 6A). Stimulation by ATP or I/F only slightly further increased G (Fig. 6B). Notably, CFTR-conductance ($G_{I/F}$) in HEK293 cells was attenuated by coexpression of TMEM16A (Fig. 6C). Taken together these data indicate an inverse relationship between CFTR and TMEM16A in HEK293 cells.

Membrane localized CFTR and TMEM16A may physically interact

The results suggest that CFTR and TMEM16A functionally interact. Both CFTR and TMEM16A are clearly membrane localized, which could allow for direct protein interaction (Fig. 7A) [18, 25]. Colocalization of both proteins was suggested by the high Spearman rank correlation coefficient of 0.83±0.13 (n = 11; c.f. methods). We found that TMEM16A was coimmunoprecipitated with CFTR in HEK293 cells, which provides some evidence for a direct physical interaction of both proteins (Fig. 7B). However, CFTR and TMEM16F did not coimmunoprecipitate when expressed in HEK293 cells, providing hints for a specific interaction of CFTR and TMEM16A (Fig. 7C).

cAMP-dependent stimulation affects intracellular Ca^{2+} signaling in HEK293 cells

Because CFTR may also affect activation of TMEM16A by changing intracellular Ca^{2+} signaling, we measured ATP- and ionomycin-induced increase of intracellular peak and plateau $[Ca^{2+}]$ using Fura2 (Fig. 8). We were unable to detect an effect of IBMX/forskolin (I/F) on ATP-induced $[Ca^{2+}]_i$ increase in cells coexpressing CFTR and TMEM16A (Fig. 8A-C). In

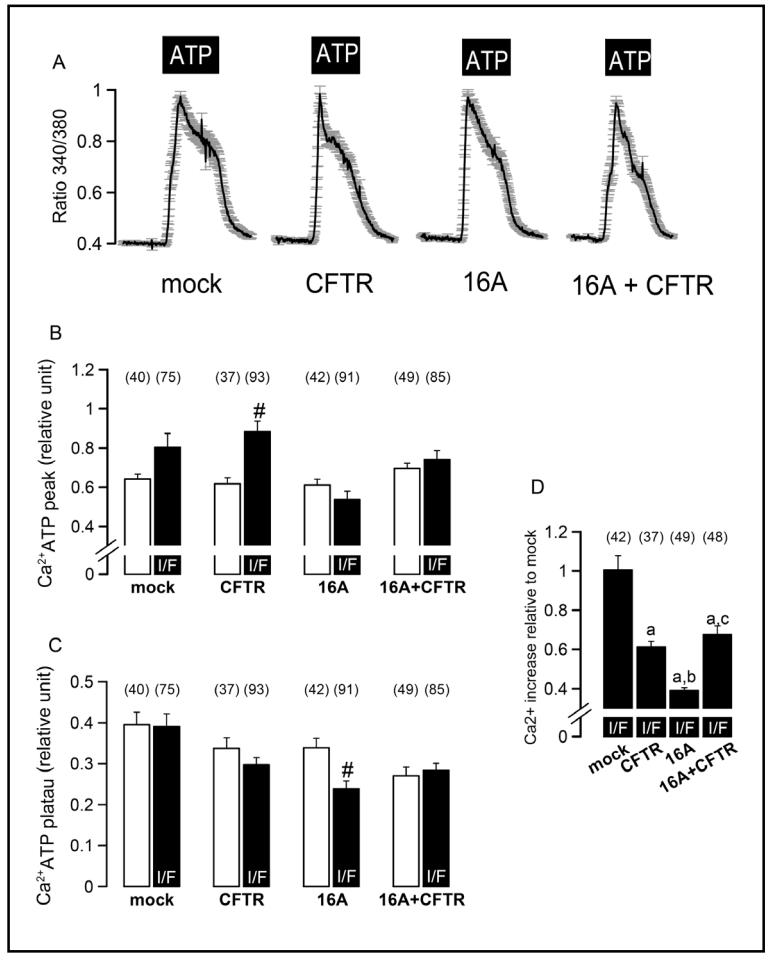

Fig. 8. cAMP-dependent stimulation affects intracellular Ca^{2+} signaling in HEK293 cells. A) ATP induced changes in $[Ca^{2+}]_i$ in mock transfected HEK293 cells and cells transiently overexpressing CFTR, TMEM16A (16A), or both proteins. B) Summary of ATP-induced peak $[Ca^{2+}]_i$ increase in the presence or absence of I/F. C) Summary of ATP-induced plateau $[Ca^{2+}]_i$ increase in the presence or absence of I/F. D) Summary of ionomycin-induced (1 μM) $[Ca^{2+}]_i$ increase in the presence of I/F. Mean ± SEM, (n) = number of cells measured. # significant difference compared to the absence of I/F (unpaired t-test). Significant difference when compared to mock ([a]), CFTR ([b]), or TMEM16A ([c]) expressing cells (ANOVA).

contrast ionomycin induced peak $[Ca^{2+}]_i$ increase was significantly reduced in cells expressing CFTR or TMEM16A (Fig. 8D). Inhibition of $[Ca^{2+}]_i$ increase during activation of TMEM16A or CFTR is possibly due to depolarization of the membrane voltage [31]. Activation of CFTR may thereby reduce the driving force for Ca^{2+} influx and attenuate activation of TMEM16A [31]. Taken together, the present results indicate that CFTR and TMEM16A are functionally related and maybe physically interact with each other.

Discussion

Enhanced CaCC in CF epithelial cells and inhibition of CaCC due to acute stimulation of CFTR implies that both Cl^- channels are somehow related [2-4]. Previously, a more detailed examination of this relationship was hampered by the fact that the molecular nature of CaCC was unknown. With identification of TMEM16A as a crucial component of CaCC [18-20] and demonstration of its intrinsic role for Ca^{2+} dependent Cl^- transport [21, 22], we are now able to re-examine this relationship. Interestingly, and similar to Namkung et al [32], we also found that siRNA-knockdown of TMEM16A in HT_{29} colonic carcinoma cells suppressed only 20 % of CaCC. In contrast, siRNA-knockdown of TMEM16A in 16HBE, CFBE (airways), CFPAC (pancreas), MDCK (kidney), and Cal-33 (stroma) cells almost completely abolished Ca^{2+} activated Cl^- conductance. Therefore we assume that TMEM16A plays the dominating role for epithelial Ca^{2+} activated Cl^- channels in most, but not all epithelial tissues. The present data now clearly show that Cl^- currents generated by TMEM16A and activated by receptor stimulation or by Ca^{2+} ionophores, are inhibited by CFTR. We found that similar to purinergic activation, also muscarinic activation of TMEM16A was inhibited during stimulation of CFTR (data not shown). The present data COIP-data supply some evidence for a direct molecular interaction of CFTR and TMEM16A.

The data obtained for ionophore-mediated activation of TMEM16A, also point to a functional interaction of

CFTR and TMEM16A. Thus ionophore-induced increase in $[Ca^{2+}]_i$ was significantly attenuated in the presence of CFTR and after stimulation with I/F, which may impede activation of TMEM16A (Fig. 8). Along this line it is interesting to note that in colonic epithelial cells the contribution of Ca^{2+} activated SK4 K^+ channels to total cellular K^+ conductance is high under control (resting) conditions, but is reduced after cAMP-dependent stimulation of the cells [33]. This is due to the cellular depolarization, causing a reduced driving force for Ca^{2+} influx and attenuated activation of TMEM16A, after cAMP-dependent stimulation. Surprisingly, attenuated increase in $[Ca^{2+}]_i$ after stimulation with IBMX/forskolin was also observed in cells expressing TMEM16A only. However, these attenuated Ca^{2+} signals did not lower TMEM16A currents (data not shown). It is therefore uncertain whether attenuated $[Ca^{2+}]_i$ signals, as measured by Fura-2, really lead to attenuated TMEM16A-currents. We found earlier that local compartmentalized intercellular Ca^{2+} concentrations control Cl^- and K^+ channels, rather that global cytosolic Ca^{2+} levels [34].

The team by Nilus and coworkers concluded that the C-terminal part of the R-domain, but not the PDZ binding motif of CFTR is involved in the interaction with endogenous Ca^{2+} -activated Cl^- channels in endothelial cells [35]. We confirmed this result by expressing a PDZ binding motif-mutant in *Xenopus* oocytes, which was still able to inhibit CaCC (data not shown). It is known that CFTR interacts with numerous proteins, many of them are receptors or have a function in cellular signaling [36]. It is entirely possible that crosstalk of CFTR with these signaling proteins contributes to inhibition of TMEM16A by CFTR.

Acknowledgements

The present work was supported by Mukoviszidose e.V. (Projekt-Nr.: S02/10), DFG SFB699/A6, and TargetScreen2 (EU-FP6-2005-LH-037365). We gratefully acknowledge the technical help with the real time PCR by Dr. F. Aldehni.

References

1 Kunzelmann K, Schreiber R: CFTR, a regulator of channels. J Membr Biol 1999;168:1-8.

2 Kunzelmann K, Mall M, Briel M, Hipper A, Nitschke R, Ricken S, Greger R: The cystic fibrosis transmembrane conductance regulator attenuates the endogenous Ca^{2+} activated Cl- conductance in Xenopus ooyctes. Pflügers Arch 1997;434:178-181.

3 Wei L, Vankeerberghen A, Cuppens H, Eggermont J, Cassiman JJ, Droogmans G, Nilius B: Interaction between calcium-activated chloride channels and the cystic fibrosis transmembrane conductance regulator. Pflugers Arch 1999;438:635-641.

4 Wei L, Vankeerberghen A, Cuppens H, Cassiman JJ, Droogmans G, Nilius B: The C-terminal part of the R-domain, but not the PDZ binding motif, of CFTR is involved in interaction with Ca^{2+} -activated Cl^- channels. Pflügers Arch 2001;442:280-285.

5 Perez-Cornejo P, Arreola J: Regulation of Ca^{2+}-activated chloride channels by cAMP and CFTR in parotid acinar cells. Biochem Biophys Res Commun 2004;316:612-617.

6 Vennekens R, Trouet D, Vankeerberghen A, Voets T, Cuppens H, Eggermont J, Cassiman JJ, Droogmans G, Nilius B: Inhibition of volume-regulated anion channels by expression of the cystic fibrosis transmembrane conductance regulator. J Physiol (Lond) 1999;515:75-85.

7 Kunzelmann K, Allert N, Kubitz R, Breuer WV, Cabantchik ZI, Normann C, Schumann S, Leipziger J, Greger R: Forskolin- and PMA-pretreatment alter the acute electrical response of HT29 cells to cAMP, ATP, neurotensin, ionomycin and hypotonic cell swelling. Pflügers Arch 1994;428:76-83.

8 Anderson MP, Welsh MJ: Calcium and cAMP activate different chloride channels in the apical membrane of normal and cystic fibrosis epithelia. Proc Natl Acad Sci USA 1991;88:6003-6007.

9 Clarke LL, Boucher RC: Chloride secretory response to extracellular ATP in human normal and cystic fibrosis nasal epithelia. Am J Physiol 1992;263:C348-C356.

10 Mall M, Gonska T, Thomas J, Schreiber R, Seydewitz HH, Kuehr J, Brandis M, Kunzelmann K: Modulation of Ca^{2+} activated Cl- secretion by basolateral K^+ channels in human normal and cystic fibrosis airway epithelia. Pediatric Research 2003;53:608-618.

11 Grubb BR, Vick RN, Boucher RC: Hyperabsorption of Na^+ and raised Ca^{2+} mediated Cl- secretion in nasal epithelia of CF mice. Am J Physiol 1994;266:C1478-C1483.

12 Clarke LL, Grubb BR, Yankaskas JR, Cotton CU, McKenzie A, Boucher RC: Relationship of a non-cystic fibrosis transmembrane conductance regulator-mediated chloride conductance to organ-level didease in cftr-/- mice. Proc Natl Acad Sci USA 1994;91:479-483.

13 Rozmahel R, Wilschanski M, Matin A, Plyte S, Oliver M, Auerbach W, Moore A, Forstner J, Durie P, Nadeau J, Bear C, Tsui LC: Modulation of disease severity in cystic fibrosis transmembrane conductance regulator deficient mice by a secondary genetic factor. Nat Genet 1996;12:280-287.

14 Ritzka M, Stanke F, Jansen S, Gruber AD, Pusch L, Woelfl S, Veeze HJ, Halley DJ, Tummler B: The CLCA gene locus as a modulator of the gastrointestinal basic defect in cystic fibrosis. Hum Genet 2004;115:483-491.

15 Loewen ME, Forsyth GW: Structure and function of CLCA proteins. Physiol Rev 2005;85:1061-1092.

16 Patel AC, Brett TJ, Holtzman MJ: The role of CLCA proteins in inflammatory airway disease. Annu Rev Physiol 2009;71:425-449.

17 Hamann M, Gibson A, Davies N, Jowett A, Walhin JP, Partington L, Affleck K, Trezise D, Main M: Human ClCa1 modulates anionic conduction of calcium-dependent chloride currents. J Physiol 2009;587:2255-2274.
18 Yang YD, Cho H, Koo JY, Tak MH, Cho Y, Shim WS, Park SP, Lee J, Lee B, Kim BM, Raouf R, Shin YK, Oh U: TMEM16A confers receptor-activated calcium-dependent chloride conductance. Nature 2008;455:1210-1215.
19 Schroeder BC, Cheng T, Jan YN, Jan LY: Expression cloning of TMEM16A as a calcium-activated chloride channel subunit. Cell 2008;134:1019-1029.
20 Caputo A, Caci E, Ferrera L, Pedemonte N, Barsanti C, Sondo E, Pfeffer U, Ravazzolo R, Zegarra-Moran O, Galietta LJ: TMEM16A, A Membrane Protein Associated With Calcium-Dependent Chloride Channel Activity. Science 2008;322:590-594.
21 Ousingsawat J, Martins JR, Schreiber R, Rock JR, Harfe BD, Kunzelmann K: Loss of TMEM16A causes a defect in epithelial Ca^{2+} dependent chloride transport. J Biol Chem 2009;284:28698-28703.
22 Rock JR, O'Neal WK, Gabriel SE, Randell SH, Harfe BD, Boucher RC, Grubb BR: Transmembrane protein 16A (TMEM16A) is a Ca^{2+} regulated Cl^- -secretory channel in mouse airways. J Biol Chem 2009;284:14875-14880.
23 Bebok Z, Collawn JF, Wakefield J, Parker W, Li Y, Varga K, Sorscher EJ, Clancy JP: Failure of cAMP agonists to activate rescued deltaF508 CFTR in CFBE41o- airway epithelial monolayers. J Physiol 2005;569:601-615.
24 Almaca J, Tian Y, AlDehni F, Ousingsawat J, Kongsuphol P, Rock JR, Harfe BD, Schreiber R, Kunzelmann K: TMEM16 proteins produce volume regulated chloride currents that are reduced in mice lacking TMEM16A. J Biol Chem 2009;284:28571-28578.
25 Schreiber R, Uliyakina I, Kongsuphol P, Warth R, Mirza M, Martins JR, Kunzelmann K: Expression and Function of Epithelial Anoctamins. J Biol Chem 2010;285:7838-7845.
26 Schultz BD, Takahashi A, Liu C, Frizzell RA, Howard M: FLAG epitope positioned in an external loop preserves normal biophysical properties of CFTR. Am J Physiol 1997;273:C2080-C2089.
27 Cozens AL, Yezzi MJ, Kunzelmann K, Ohrui T, Chin L, Eng K, Finkbeiner WE, Widdicombe JH, Gruenert DC: CFTR expression and chloride secretion in polarized immortal human bronchial epithelial cells. Am J Respir Cell Mol Biol 1994;10:38-47.
28 Bruscia E, Sangiuolo F, Sinibaldi P, Goncz KK, Novelli G, Gruenert DC: Isolation of CF cell lines corrected at DeltaF508-CFTR locus by SFHR-mediated targeting. Gene Ther 2002;9:683-685.
29 Kunzelmann K, Kongsuphol P, AlDehni F, Tian Y, Ousingsawat J, Warth R, Schreiber R: Bestrophin and TMEM16 - Ca^{2+} activated Cl^- channels with different functions. Cell Calcium 2009;46:233-241.
30 de la Fuente R, Namkung W, Mills A, Verkman AS: Small molecule screen identifies inhibitors of a human intestinal calcium activated chloride channel. Mol Pharmacol 2007;73:758-768.
31 Fischer KG, Leipziger J, Rubini-Illes P, Nitschke R, Greger R: Attenuation of stimulated Ca^{2+} influx in colonic epithelial (HT29) cells by cAMP. Pflugers Arch 1996;432:735-740.
32 Namkung W, Phuan PW, Verkman AS: TMEM16A inhibitors reveal TMEM16A as a minor component of CaCC conductance in airway and intestinal epithelial cells. J Biol Chem 2011;286:2365-2374.
33 Heitzmann D, Warth R: Physiology and pathophysiology of potassium channels in gastrointestinal epithelia. Physiol Rev 2008;88:1119-1182.
34 Kunzelmann K, Kongsuphol P, Chootip K, Toledo C, Martins JR, Almaca J, Tian Y, Witzgall R, Ousingsawat J, Schreiber R: Role of the Ca^{2+}-activated Cl^- channels bestrophin and anoctamin in epithelial cells. Biol Chem 2011;392:125-134.
35 Serohijos AW, Hegedus T, Aleksandrov AA, He L, Cui L, Dokholyan NV, Riordan JR: Phenylalanine-508 mediates a cytoplasmic-membrane domain contact in the CFTR 3D structure crucial to assembly and channel function. Proc Natl Acad Sci USA 2008;105:3256-3261.
36 Guggino WB, Stanton BA: New insights into cystic fibrosis: molecular switches that regulate CFTR. Nat Rev Mol Cell Biol 2006;7:426-436.